

***Ab initio* study of charge transfer in low energy Si²⁺ collisions with atomic hydrogen**

N J Clarke^{†¶}, P C Stancil^{‡+}, B Zygelman^{§*} and D L Cooper^{||‡}

[†] School Of Chemistry, University Of Birmingham, Edgbaston, Birmingham B15 2TT, UK

[‡] Physics Division, Oak Ridge National Laboratory, PO Box 2008, Oak Ridge, TN 37831-6372, USA

[§] W M Keck Laboratory for Computational Physics, Department of Physics, University of Nevada, Las Vegas, NV 89154-4002, USA

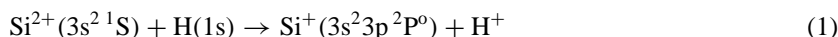
^{||} Department of Chemistry, University of Liverpool, PO Box 147, Liverpool L69 7ZD, UK

Received 3 September 1997

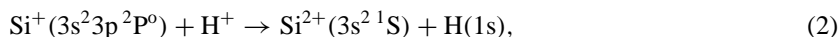
Abstract. Charge transfer cross sections for collisions of ground state Si²⁺(3s²1S) and excited state Si²⁺(3s3p³P^o) with atomic hydrogen are presented for energies less than 100 eV amu⁻¹. The cross sections are calculated in a diabatic representation using a fully quantum-mechanical, molecular-orbital, close-coupled method. Completely *ab initio* adiabatic potentials and nonadiabatic radial coupling matrix elements obtained with the spin-coupled valence-bond method are incorporated. Inclusion of the Si⁺(3s3p²2D) + H⁺ and Si²⁺(3s3p³P^o) + H(1s) closed-channels results in oscillations in the Si²⁺(3s²1S) charge transfer cross section for collision energies above the separated-atom energy of the lowest closed-channel (~ 4.2 eV amu⁻¹). Rate coefficients for temperatures between 500 and 100 000 K and cross sections for collisions with isotopic D are presented. Results for the reverse process, charge transfer ionization, are also given.

1. Introduction

The charge transfer process



has been previously investigated by Bates and Moiseiwitsch (1954), using the Landau–Zener approximation and with a quantal, close-coupled, model potential approach by McCarroll and Valiron (1976) and Gargaud *et al* (1982). Reaction (1) is an important recombination mechanism for Si²⁺ in diffuse interstellar clouds. Process (1), and its reverse, the charge transfer ionization reaction



which is endothermic by $\Delta E = 2.74$ eV, have been shown by Baliunas and Butler (1980), for coronal plasmas, and by Butler and Raymond (1980), for low-velocity shocks, to be crucial in determining the silicon ionization balance. It is therefore essential to have an accurate estimate of the rate coefficient of reaction (1). For that purpose, we present

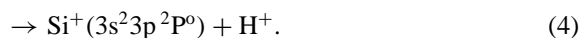
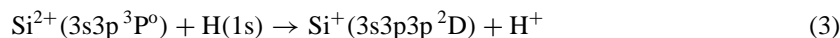
¶ E-mail address: nickc@tccp.bham.ac.uk

⁺ Eugene P Wigner Fellow. E-mail address: stancil@mail.phy.ornl.gov

^{*} E-mail address: bernard@physics.unlv.edu

[‡] E-mail address: dlc@rs2.ch.liv.ac.uk

an *ab initio* investigation of process (1) in which the scattering equations are solved in the diabatic representation through a fully quantum-mechanical, molecular-orbital, close-coupled approach (see for example Zygelman *et al* 1992). We include only radial coupling since Gargaud *et al* (1982) have shown that rotational coupling contributes negligibly below ~ 100 eV. We further include the closed channels $\text{Si}^+(3s3p^2^2\text{D}) + \text{H}^+$ and $\text{Si}^{2+}(3s3p^3\text{P}^0) + \text{H}(1s)$ which are endothermic by 4.11 and 6.54 eV, respectively, investigate the isotope dependence for deuterium targets and present the first analysis of electron capture by the $\text{Si}^{2+}(3s3p^3\text{P}^0)$ metastable state:



Atomic units are used throughout unless stated otherwise.

2. SCVB calculations

The adiabatic potentials and nonadiabatic radial couplings are obtained through the spin-coupled valence-bond (SCVB) method (see for example Cooper *et al* 1988). Since this is a fully flexible *ab initio* technique, the close nuclear separation (molecular) region is described with the same accuracy as is the asymptotic separated-atom limit. The model potential approach of Gargaud *et al* (1982) incorporates adjustable parameters which enable the potentials to have the correct separated-atom behaviour, but may not describe the molecular region very accurately.

We adopt Dunning correlation-consistent basis sets of triple- ζ -valence quality for Si/H consisting of (15s9p2d/5s2p) Gaussian-type orbitals contracted to [5s4p2d/3s2p]. SCVB expansions were performed in the space of the three valence electrons, with the $\text{Si}(1s^22s^22p^6)$ core described by optimized molecular orbitals taken from state-averaged, full-valence, complete-active-space self-consistent field (CASSCF) calculations. The SCVB structures consist of all single and double excitations plus all singly ionic cross excitations. These excitations are from the ground and first excited states into a set of three σ and two π virtual orbitals for each valence electron plus one δ virtual orbital for each of the $\text{Si}(3s3s')$ electrons. A carefully selected set of additional cross excitations were added to refine the description of the $3^2\Sigma^+$ state, giving a total of just 230 spatial configurations. Further details including CASSCF and spin-coupled potentials can be found in Clarke (1995) and Clarke *et al* (1997).

The resulting adiabatic potentials, evaluated at 80 internuclear separations R between 2.2 and $18 a_0$, are given in figure 1. The $1^2\Sigma^+$ and $2^2\Sigma^+$ potentials are in reasonable agreement with those of Gargaud *et al* (1982). Park and Sun (1993), using an effective valence shell Hamiltonian method, calculated adiabatic potentials for the $1^2\Sigma^+$, $2^2\Sigma^+$, $3^2\Sigma^+$, and $4^2\Sigma^+$ states which are in fair agreement with the current results. A comparison of experimental with theoretical separated-atom energies is given in table 1. The deviation of the current results from the measured energies is between only 2 and 5.5%. Table 2 gives the avoided crossing distances R_x and the corresponding adiabatic potential differences ΔU_x at R_x . For the $1^2\Sigma^+ - 2^2\Sigma^+$ avoided crossing, the current R_x is larger and the ΔU_x smaller than obtained in the previous calculations. Our results agree well with the data of Park and Sun (1993) for the $2^2\Sigma^+ - 3^2\Sigma^+$ avoided crossing; whereas for the $3^2\Sigma^+ - 4^2\Sigma^+$ case, we find $R_x = 12.84 a_0$ which is in disagreement with Park and Sun (1993) whose results imply that the crossing distance is much larger than $13 a_0$. Consideration of the relative separated-atom energies of these states suggests $R_x < 13 a_0$. The $2^2\Sigma^+$ state which correlates to the $\text{Si}^+(3s^24s^2\text{S}) + \text{H}^+$ asymptotic separated-atom channel has an avoided crossing with the

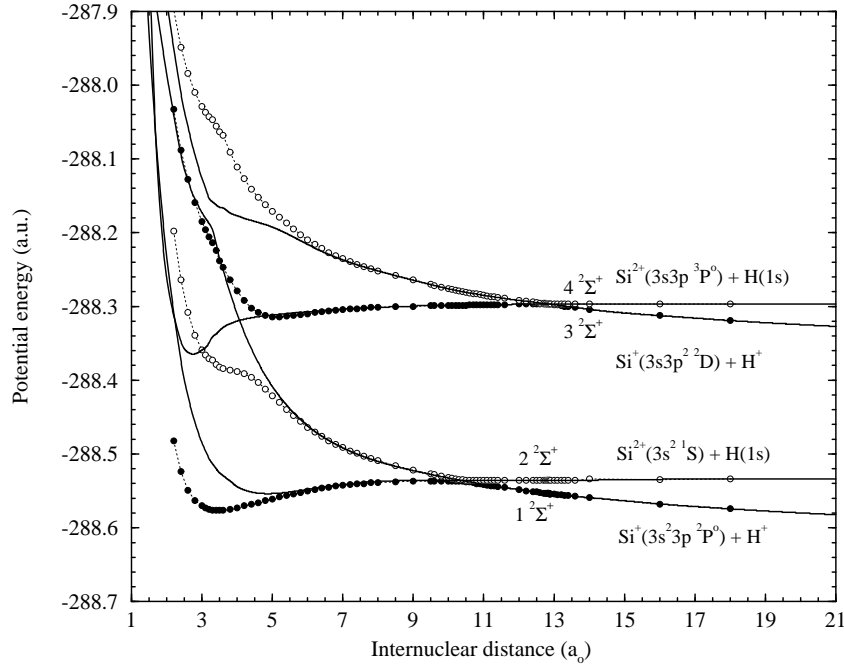


Figure 1. The $^2\Sigma^+$ adiabatic (circles) and diagonal diabatic (—) potential energies for the SiH^{2+} system as a function of internuclear distance R .

Table 1. Asymptotic separated-atom energies for the $^2\Sigma^+$ states of SiH^{2+} .

Molecular state	Asymptotic atomic states	Energy (eV)	
		Theory	Expt ^a
$1^2\Sigma^+$	$\text{Si}^+(3s^2 3p^2 P^0) + \text{H}^+$	-2.613	-2.74
$2^2\Sigma^+$	$\text{Si}^{2+}(3s^2 1S) + \text{H}(1s)$	0.00	0.00
$3^2\Sigma^+$	$\text{Si}^+(3s3p^2 D) + \text{H}^+$	4.333	4.11
$^2\Sigma^+$	$\text{Si}^+(3s^2 4s^2 S) + \text{H}^+$	—	5.49
$4^2\Sigma^+$	$\text{Si}^{2+}(3s3p^3 P^0) + \text{H}(1s)$	6.451	6.54

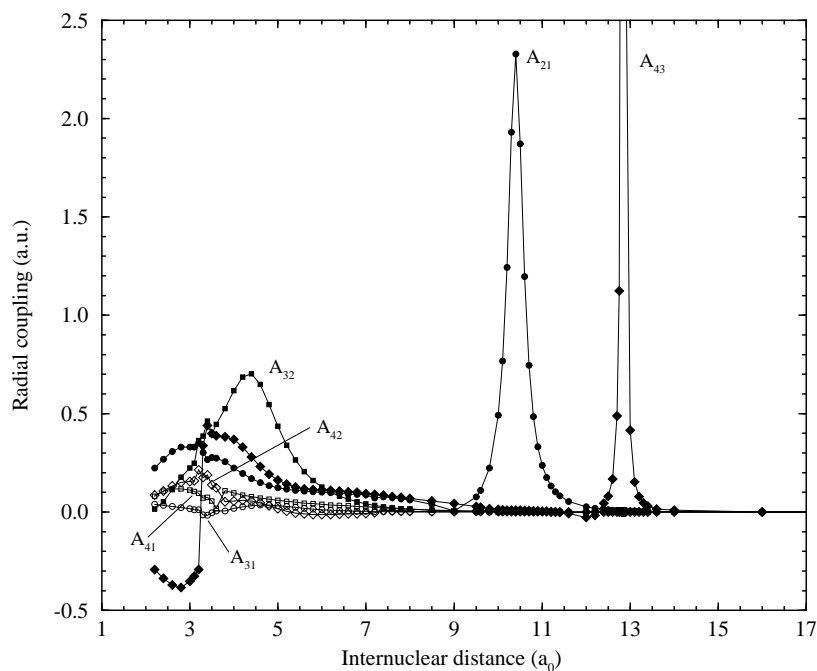
^a Baskin and Stoner (1975).

$4^2\Sigma^+$ state near $26 a_0$ with, probably, a very small ΔU_x . As this channel is expected to give a negligible contribution to the total cross section, since a very small adiabatic energy difference implies nearly diabatic behaviour, we have not calculated it.

The nonadiabatic radial couplings are displayed in figure 2. The A_{21} coupling is in fair agreement with Gargaud *et al* (1982), except that their coupling has a phase change for $R < 8 a_0$. We impose a phase change if a coupling approaches zero with a sufficiently large gradient, which is not justified in the case of A_{21} . We are unaware of other calculations for the other radial couplings. Given the nonadiabatic couplings, we transform to a diabatic basis by a unitary transformation to eliminate first-order derivatives (see for example Zygelman *et al* 1992). The diagonal elements of the resulting diabatic potential matrix are displayed in figure 1 while the off-diagonal elements are given in figure 3.

Table 2. Avoided crossings and adiabatic potential differences at avoiding crossings for the $^2\Sigma^+$ states of SiH^{2+} .

Molecular states	R_x (au)	ΔU_x (eV)
$1^2\Sigma^+ - 2^2\Sigma^+$	9.93 ^a	0.131 ^a
	9.75 ^b	0.080 ^b
	$\sim 10^c$	—
	10.4 ^d	0.052 ^d
$2^2\Sigma^+ - 3^2\Sigma^+$	3.53 ^a	$\sim 1.2^a$
	$\sim 4.5^c$	$\sim 2.7^c$
	4.4 ^d	2.57 ^d
$3^2\Sigma^+ - 4^2\Sigma^+$	11.21 ^a	0.046 ^a
	$> 13^c$	—
	12.84 ^d	0.0033 ^d

^a From empirical potentials obtained using procedures of Butler and Dalgarno (1980).^b From model potentials, McCarroll and Valiron (1976) and Gargaud *et al* (1982).^c From *ab initio* potentials, Park and Sun (1993).^d From *ab initio* potentials, this work.**Figure 2.** The $^2\Sigma^+$ nonadiabatic radial couplings for the SiH^{2+} system as a function of internuclear distance R .

3. Results and discussion

The calculations were performed in the perturbed-stationary-state approximation using a fully quantum-mechanical, molecular-orbital, close-coupled approach previously described

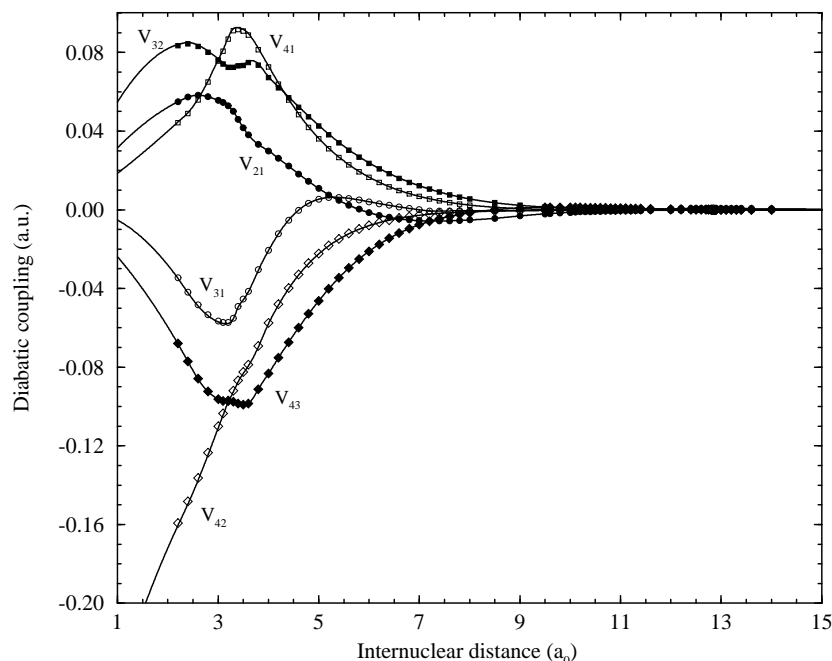


Figure 3. The $2^2\Sigma^+$ off-diagonal diabatic potentials for the SiH^{2+} system as a function of internuclear distance R .

in Zygelman *et al* (1992) where the coupled scattering equations are integrated using an implementation of the log-derivative method of Johnson (1973). All four channels were included except when the incident channel was either the $1^2\Sigma^+$ or $2^2\Sigma^+$ state and the collision energy was less than the asymptotic energy of the $3^2\Sigma^+$ state, in which case a two-channel calculation was performed. Electron translation factors, which are often included to remove asymptotic couplings between atomic states that are connected by dipole transitions, were not included. For the current system, the $2^2\Sigma^+$ and $4^2\Sigma^+$ states are dipole-coupled through a weak intercombination dipole moment of $\sim 0.01 ea_0$, while the asymptotic dipole moment coupling the $1^2\Sigma^+$ and $3^2\Sigma^+$ states is $\sim 0.07 ea_0$. The neglect of these asymptotic couplings should have a negligible effect for the currently investigated energy range.

3.1. Electron capture by the $\text{Si}^{2+}(3s^2\ ^1S)$ ground state

Charge transfer cross sections for process (1) are presented in figure 4. The present results, which are given over a much finer collision energy grid than previous studies, are in fair agreement with the model potential calculations of McCarroll and Valiron (1976) and Gargaud *et al* (1982) though they lack the inflection near 0.5 eV amu^{-1} present in the earlier results. A Landau-Zener analysis suggests that the cross section is very sensitive to the value of ΔU_x which varied significantly between the various calculations (see table 2). The amplitude of the oscillatory structures present in the cross section below $\sim 0.1 \text{ eV amu}^{-1}$ and their energy are sensitive to the smoothness and location of the fit of the *ab initio* diagonal diabatic potentials to the asymptotic long-range form. State-selective cross sections for capture into the $\text{Si}^+(^2D)$ state are shown in figure 5. This process, which is endothermic by 4.11 eV, is unimportant for the considered energy range, but may play a role at high

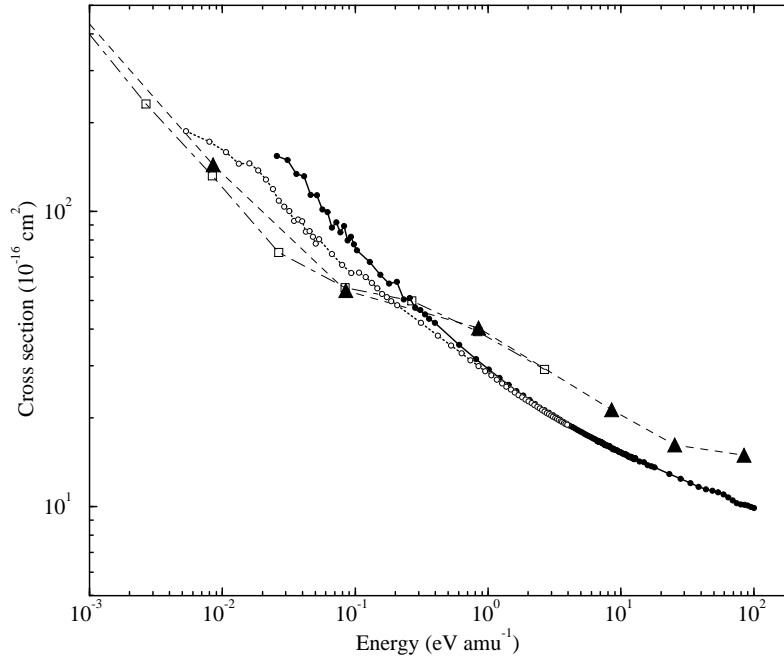


Figure 4. Total electron capture cross sections from the ground state $\text{Si}^{2+}(3s^2\ ^1S)$. $\text{Si}^{2+} + \text{H}$: this work (full circles), Gargaud *et al* (1982) (triangles), and McCarroll and Valiron (1976) (squares). $\text{Si}^{2+} + \text{D}$: this work (open circles).

energies. For H targets, this corresponds to a threshold of 4.2 eV amu^{-1} and 2.2 eV amu^{-1} for D targets as indicated in figure 5. The cross section for this weak channel may be somewhat larger as a consequence of rotational coupling.

In table 3, we present rate coefficients for the electron-capture process (1) which were determined by averaging over the cross sections with a Maxwellian velocity distribution. The rates are fitted to the parametric form

$$\alpha(T) = \sum_i a_i \left(\frac{T}{10\,000} \right)^{b_i} \exp \left(\frac{-T}{c_i} \right) \quad (5)$$

with the parameters a_i ($\text{cm}^3 \text{ s}^{-1}$), b_i , and c_i (K) given at the bottom of table 3. The fits are reliable to within 10% except for the fit for reaction (4) which is only accurate to within 30%. Our quantal rate coefficients, presented in figure 6, do not agree with either the Landau–Zener calculations of Bates and Moiseiwitsch (1954) or the quantal, close-coupling results of McCarroll and Valiron (1976) and Gargaud *et al* (1982). This discrepancy is a direct consequence of the fact that the current cross sections are smaller than the previous works for $E > 0.3 \text{ eV amu}^{-1}$; this is related to the differences in ΔU_x and R_x obtained by the various authors. Measurements in this energy or temperature range are needed.

3.2. Target isotope dependence

Stancil and Zygelman (1995) have discussed the influence of an isotope effect on the total low energy charge transfer cross section, an effect which was recently verified by a merged-beams measurement of Si^{4+} with D (Pieksma *et al* 1996). From the Landau–

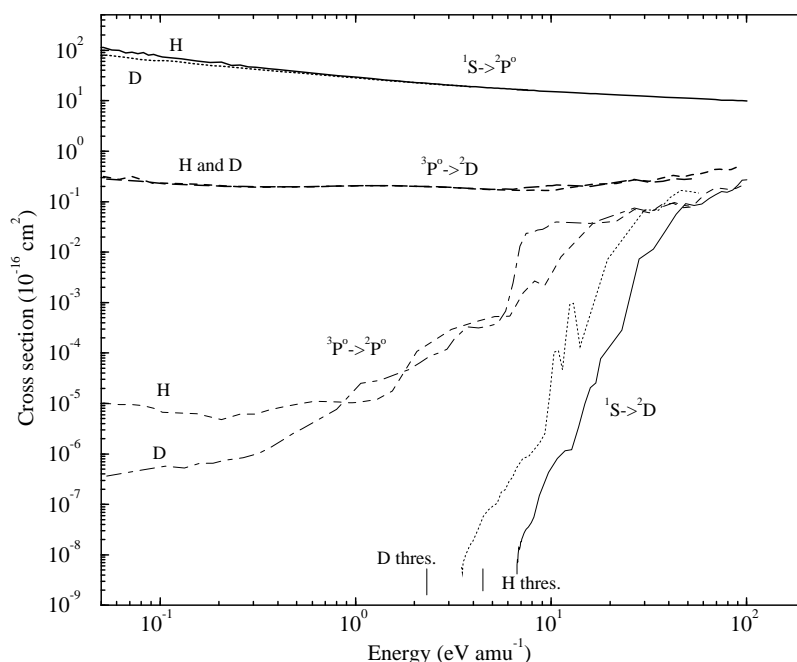


Figure 5. Electron-capture cross sections for processes (1), (3), and (4) with H and D targets. The initial Si^{2+} and final Si^+ states are indicated in the figure and the energy scale refers to the center-of-mass collision energy in the entrance channel.

Zener approximation, Stancil and Zygelman (1995) derived a formula to relate the thermal energy D target and H target cross sections:

$$\frac{\sigma(\text{H})}{\sigma(\text{D})} \approx \frac{1 - 2V_{22}/\mu(\text{H})v^2}{1 - 2V_{22}/\mu(\text{D})v^2} \quad (6)$$

where V_{22} is the diabatic potential of the entrance channel, μ is the reduced mass of the isotopic quasi-molecule, and v the collision velocity in the centre-of-mass frame. Equation (6) predicts a threshold for the isotope effect of $\sim 0.4 \text{ eV amu}^{-1}$ and $\sigma(\text{H})/\sigma(\text{D}) \sim 1.07$ at 0.1 eV amu^{-1} . We define the threshold as the energy at which the H target cross section is 2% larger than the D target cross section. The quantum calculation, shown in figure 4, gives a threshold of $\sim 1 \text{ eV amu}^{-1}$ and $\sigma(\text{H})/\sigma(\text{D}) \sim 1.2$ at 0.1 eV amu^{-1} .

Rate coefficients for reaction (1) with D targets are given in table 4 and figure 6. Also shown in figure 6 are the rate coefficients for D targets, but calculated from the H target cross section by scaling the collision energy with the reduced masses. The discrepancy reaches a maximum of 20% near 1000 K.

Figure 7 presents partial cross sections σ_J versus total angular momentum J for reaction (1) with H and D targets at 0.05 and 50 eV amu^{-1} . At 50 eV amu^{-1} , the number of contributing partial waves for a D target is nearly twice that for the H target as shown in figure 7(b). However, the magnitude of the D target partial cross sections are about half the magnitude of the H partial cross sections, with the net result of a target-mass-independent total cross section. For the lower collision energy of 0.05 eV amu^{-1} , displayed in figure 7(a), the number of contributing partial cross sections for the D target is again about twice that of the H target. However, the H target partial cross sections are typically 2.3 times the D target values, resulting in an enhanced total H cross section. The target

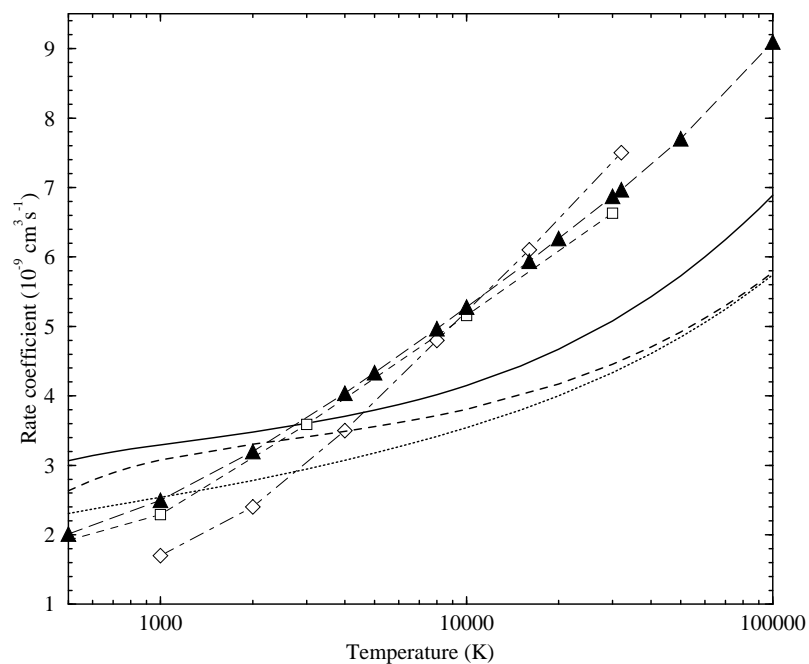


Figure 6. Electron capture rate coefficients for reaction (1). The designations are as given in figure 4 with the additions of $\text{Si}^{2+} + \text{H}$: Bates and Moiseiwitsch (1954) (diamonds) and $\text{Si}^{2+} + \text{D}$: this work, determined with the D cross section ($\cdots\cdots$) and the mass-scaled H cross section ($---$).

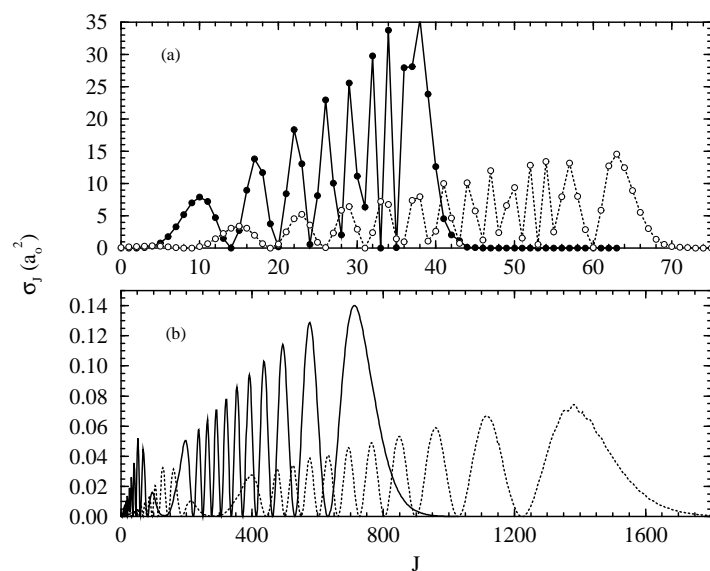


Figure 7. Partial cross sections σ_J versus J for capture into $\text{Si}^+(3s^23p^1P^o)$ from $\text{Si}^{2+}(^1S) + \text{H}$ (—) and $\text{Si}^{2+}(^1S) + \text{D}$ ($\cdots\cdots$). (a) $E = 0.05 \text{ eV amu}^{-1}$, (b) $E = 50 \text{ eV amu}^{-1}$.

Table 3. Charge transfer rate coefficients α ($\text{cm}^3 \text{s}^{-1}$) for H targets as a function of temperature T . Fitting parameters a_i ($\text{cm}^3 \text{s}^{-1}$), b_i , and c_i (K) according to equation (5) are given at the end of the table.

T (K)	Reaction			
	1	2	3	4
500	3.06–9 ^a	—	—	—
700	3.19–9	—	—	—
900	3.27–9	—	—	—
1 000	3.30–9	—	9.31–12	2.85–16
2 000	3.48–9	3.0–16	1.33–11	4.98–16
4 000	3.70–9	6.3–13	1.88–11	1.37–15
6 000	3.87–9	8.2–12	2.30–11	4.12–15
8 000	4.02–9	1.7–11	2.64–11	9.21–15
10 000	4.15–9	6.7–11	2.93–11	1.67–14
15 000	4.43–9	2.0–10	3.49–11	5.33–14
20 000	4.67–9	3.4–10	3.93–11	1.47–13
30 000	5.08–9	6.2–10	4.65–11	6.76–13
40 000	5.43–9	8.5–10	5.29–11	1.75–12
50 000	5.73–9	1.0–9	5.90–11	3.31–12
60 000	6.00–9	1.2–9	6.48–11	5.23–12
70 000	6.25–9	1.4–9	7.05–11	7.42–12
80 000	6.48–9	1.5–9	7.61–11	9.82–12
90 000	6.69–9	1.6–9	8.16–11	1.24–11
100 000	6.89–9	1.7–9	8.70–11	1.50–11
a_1	4.04–9	—	2.87–11	1.80–14
b_1	9.40–2	—	4.72–1	2.90
c_1	–2.90+5	—	8.46+6	–2.93+5
a_2	—	—	—	7.26–17
b_2	—	—	—	–0.63
c_2	—	—	—	–1.92+5

^a The notation $A - B$ corresponds to $A \times 10^{-B}$.

mass and J dependence behaviour are similar to those noted for the Si^{4+}/He and N^{4+}/H systems by Stancil *et al* (1997a, b).

3.3. Closed-channel effects

For H target collision energies above $\sim 4.45 \text{ eV amu}^{-1}$, the system may interact with the endothermic closed channels $3^2\Sigma^+$ and $4^2\Sigma^+$. We have developed a simple approach for incorporating closed channels without using modified Bessel functions for the asymptotic solutions as described by Johnson (1973). The method will be described in a future publication (Stancil *et al* 1997c). Figure 8(a) shows that the calculated cross section neglecting the closed-channels (a two-channel calculation) is smooth and monotonically decreasing with energy. Inclusion of the closed channels (four-channel calculation) results in an oscillatory structure beginning near 4.2 eV amu^{-1} and extending up to $\sim 6.6 \text{ eV amu}^{-1}$ (the $4^2\Sigma^+$ threshold). This closed-channel oscillatory behaviour was previously observed in the Mg/H^+ charge transfer system (Allan *et al* 1988) and may be associated with predissociating bound vibrational levels of the $4^2\Sigma^+$ diabatic potential well (see for example Preston and Dalgarno 1987). The oscillations will have little effect on the rate coefficient, but they may be observable in total charge transfer measurements. A similar structure is

Table 4. Charge transfer rate coefficients α ($\text{cm}^3 \text{s}^{-1}$) for D targets as a function of temperature T . Fitting parameters a_i ($\text{cm}^3 \text{s}^{-1}$), b_i , and c_i (K) according to equation (5) are given at the end of the table.

T (K)	Reaction			
	1	2	3	4
500	2.30–9 ^a	—	—	—
700	2.42–9	—	—	—
900	2.51–9	—	—	—
1 000	2.54–9	—	5.40–12	1.26–17
2 000	2.78–9	2.4–16	9.14–12	3.60–17
4 000	3.07–9	5.2–13	1.34–11	1.82–16
6 000	3.27–9	7.0–12	1.64–11	5.55–16
8 000	3.41–9	2.6–11	1.91–11	1.18–15
10 000	3.54–9	5.7–11	2.14–11	2.13–15
15 000	3.78–9	1.7–10	2.61–11	8.73–15
20 000	4.00–9	2.9–10	2.99–11	3.73–14
30 000	4.33–9	5.3–10	3.58–11	2.72–13
40 000	4.60–9	7.2–10	4.04–11	8.25–13
50 000	4.84–9	8.8–10	4.45–11	1.65–12
60 000	5.06–9	1.0–9	4.81–11	2.66–12
70 000	5.25–9	1.1–9	5.15–11	3.79–12
80 000	5.42–9	1.2–9	5.46–11	5.02–12
90 000	5.59–9	1.3–9	5.77–11	6.31–12
100 000	5.74–9	1.4–9	6.06–11	7.64–12
a_1	3.49–9	—	2.19–11	1.19–15
b_1	1.39–1	—	5.62–1	2.13
c_1	–5.25+5	—	3.12+5	–2.89+4
a_2	—	—	—	9.92–16
b_2	—	—	—	7.31
c_2	—	—	—	1.12+4

^a The notation $A - B$ corresponds to $A \times 10^{-B}$.

present in the D target cross section, but over the range $2.2 < E < 3.5 \text{ eV amu}^{-1}$ as displayed in figure 8(b).

3.4. Electron capture by the $\text{Si}^{2+}(3s3p^3P^o)$ metastable state

Cross sections for the charge transfer reactions (3) and (4) are presented in figure 5. The cross section is fairly small and flat, varying between 2 and $5 \times 10^{-17} \text{ cm}^2$ over the considered energy range. It is dominated by capture to the $\text{Si}^+(3s3p^2D)$ state, but above $\sim 20 \text{ eV amu}^{-1}$ capture into the $\text{Si}^+(3s^23p^2P^o)$ state begins to contribute significantly. Since the metastable cross section is more than an order of magnitude smaller than the ground-state cross section, future ground-state charge transfer measurements will not be contaminated due to metastables even if the ion beam has a significant metastable component. Capture into the $\text{Si}^+(3s3p^2D)$ state has no isotope dependence, but the $\text{Si}^+(3s^23p^2P^o)$ capture cross section is smaller for D targets for collision energies below $\sim 1 \text{ eV amu}^{-1}$. Quantal rate coefficients for capture into $\text{Si}^+(3s3p^2D)$ and $\text{Si}^+(3s^23p^2P^o)$ states for H and D targets are given in tables 3 and 4, respectively.

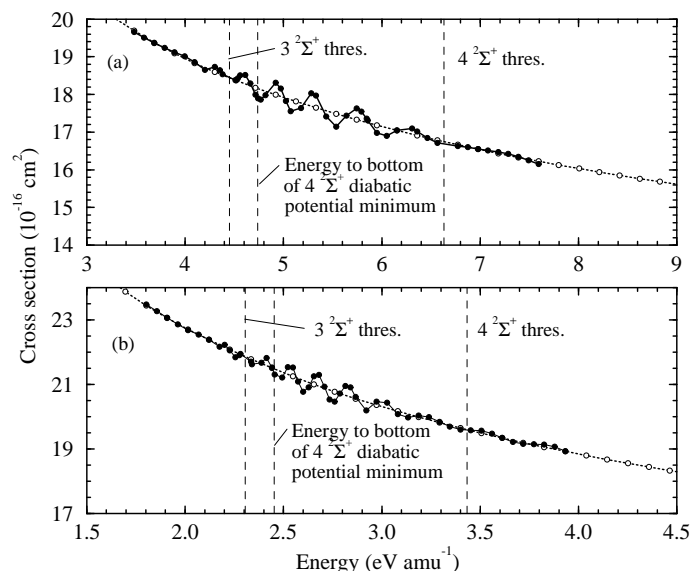


Figure 8. The effect of the closed channels on the electron-capture cross sections for reaction (1). With the closed channels (full circles), without the closed channels (open circles). (a) H targets, (b) D targets.

3.5. Charge transfer ionization

Rate coefficients $\alpha_2(T)$ for charge transfer ionization, the reverse of reaction (1), can be obtained from the detailed balance equation

$$\alpha_2(T) = \frac{1}{3} \exp(-\Delta E/kT) \alpha_1(T) \quad (7)$$

where ΔE is the asymptotic separated-atom energy defect, taken to be 2.613 eV, and α_1 is the rate coefficient for process (1). α_2 can also be calculated directly from the cross section for reaction (2) which is given in figure 9 for both H^+ and D^+ targets. The rate coefficients are given in table 3 and are typically 20% smaller than obtained by Gargaud *et al* (1982). The difference is a consequence of the discrepancy in the forward reaction (1). Rate coefficients with D^+ are given in table 4.

Cross sections for the reverse of processes (3) and (4) are given in figure 9. All of the charge transfer ionization reactions, except $\text{Si}^+(^2\text{D}) + \text{H}^+ \rightarrow \text{Si}^{2+}(^1\text{S}) + \text{H}$, are endothermic with zero cross sections below a few eV amu^{-1} . As stated above, the cross sections of the weaker channels may be enhanced if rotational coupling is considered.

4. Applications

The importance of charge transfer in astrophysical and fusion plasmas has been discussed by many authors (see for example Shields 1988, Janev 1993, Stancil *et al* 1997a, b). We briefly mention some applications particular to Si^{2+} .

In supernova remnants, charge exchange with H tends to drive the ionization stages of the metals to be singly ionized and process (1) is the last in a chain of charge transfer reactions for silicon ions.

Péquignot *et al* (1978) demonstrated that charge transfer must be included in models of planetary nebulae to explain accurately the ionization structure. The models of Clegg

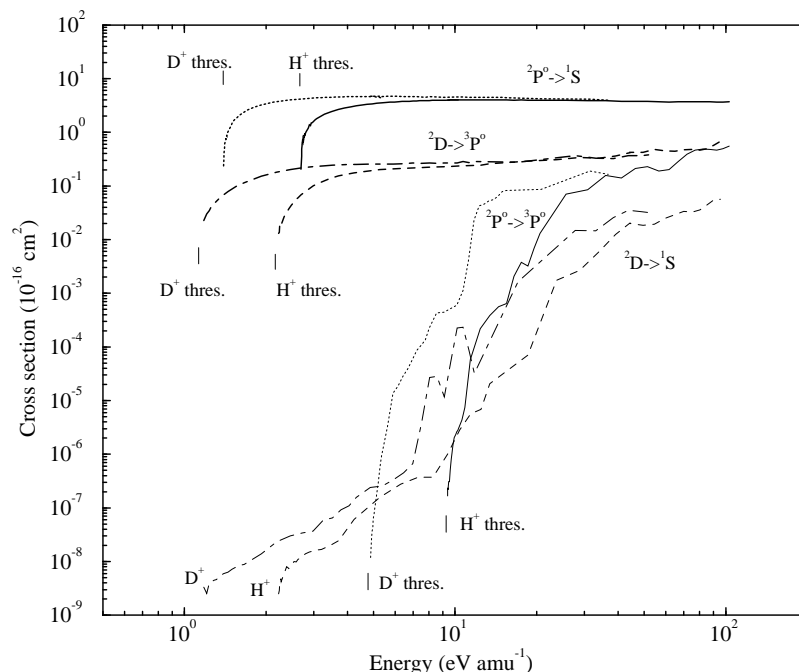


Figure 9. Charge transfer ionization cross sections: $\text{Si}^{2+} + \text{H}^+(\text{D}^+) \rightarrow \text{Si}^{3+} + \text{H}(\text{D})$. The initial Si^{2+} and final Si^{3+} states are indicated in the figure and the energy scale refers to the center-of-mass collision energy in the entrance channel.

et al (1987) used the rate coefficients of McCarroll and Valiron (1976) for reaction (1) to predict the abundance of Si^{2+} and estimate the Si III 1883/1892 Å intercombination line ratio which is used as an electron density diagnostic. For the Orion Nebula, where Si^{2+} is the dominant ionization state of silicon, Rubin *et al* (1993) incorporated the Gargaud *et al* (1982) rate coefficients in a ‘blister’ photoionization model to estimate the silicon abundance from observations of the 1883/1892 Å line. Our new rate coefficients are $\sim 25\%$ smaller at $T \sim 10\,000\text{--}20\,000$ K and may affect these models.

Charge transfer is also important in the x-ray illuminated nebulae models of Kallman and McCray (1982). Process (1) is relevant to models pertaining to interstellar gas surrounding compact galactic sources, compact sources embedded in dense interstellar clouds, and compact sources with stellar winds or accretion flows.

5. Summary

We have presented a completely *ab initio* investigation of low-energy electron capture in collisions of Si^{2+} with atomic hydrogen. Results for capture by the Si^{2+} ground state differ from previous theoretical calculations. Measurements would be helpful to resolve the discrepancy. Electron capture by the $\text{Si}^{2+}(3s3p\ ^3\text{P}^o)$ excited state have been studied for the first time and suggest that the rate coefficient is two orders of magnitude smaller than for capture by the ground state. Target isotope effects have been addressed and an interesting oscillatory structure was found due to coupling from a closed channel.

Acknowledgments

A portion of the work of PCS was performed as a Eugene P Wigner Fellow and staff member at the Oak Ridge National Laboratory, managed by Lockheed Martin Energy Research Corp for the U S Department of Energy under Contract DE-AC05-96OR22464. PCS and BZ also acknowledge support from NSF EPSCoR grant OSR-9353227 in Chemical Physics to the state of Nevada.

References

- Allan R J, Clegg R E S, Dickinson A S and Flower D R 1988 *Mon. Not. R. Astron. Soc.* **235** 1245
Baliunas S L and Butler S E 1980 *Astrophys. J. Lett.* **235** L45
Baskin S and Stoner J O Jr 1975 *Atomic Energy-levels and Grottrian Diagrams* (Amsterdam: North-Holland)
Bates D R and Moiseiwitsch B L 1954 *Proc. Phys. Soc. A* **67** 805
Butler S E and Dalgarno A 1980 *Astrophys. J.* **241** 838
Butler S E and Raymond J C 1980 *Astrophys. J.* **240** 680
Clarke N J 1995 *Doctoral Thesis* University of Liverpool
Clarke N J, Cooper D L, Gerratt J and Raimondi M 1997 in preparation
Clegg R E S, Harrington J P, Barlow M J and Walsh J R 1987 *Astrophys. J.* **314** 551
Cooper D L, Gerratt J and Raimondi M 1988 *Int. Rev. Phys. Chem.* **7** 59
Gargaud M, McCarroll R and Valiron P 1982 *Astron. Astrophys.* **106** 197
Janev R K 1993 *Review of Fundamental Processes and Applications of Atoms and Molecules* ed C D Lin (Singapore: World Scientific) p 1
Johnson B R 1973 *J. Comput. Phys.* **13** 445
Kallman T R and McCray R 1982 *Astrophys. J. Suppl.* **50** 263
McCarroll R and Valiron P 1976 *Astron. Astrophys.* **53** 83
Park J K and Sun H 1993 *J. Chem. Phys.* **99** 1844
Péquignot D, Aldrovandi S M V and Stasinska G 1978 *Astron. Astrophys.* **63** 313
Piekma M, Gargaud M, McCarroll R and Havener C C 1996 *Phys. Rev. A* **54** R13
Preston S and Dalgarno A 1987 *Chem. Phys. Lett.* **138** 157
Rubin R H, Dufour R J and Walter D K 1993 *Astrophys. J.* **413** 242
Shields G A 1988 *Molecular Astrophysics* ed T W Hartquist (Cambridge: Cambridge University Press) p 461
Stancil P C and Zygelman B 1995 *Phys. Rev. Lett.* **75** 1495
Stancil P C, Zygelman B, Clarke N J and Cooper D L 1997a *Phys. Rev. A* **55** 1064
———1997b *J. Phys. B: At. Mol. Opt. Phys.* **30** 1013
———1997c in preparation
Zygelman B, Cooper D L, Ford M J, Dalgarno A, Gerratt J and Raimondi M 1992 *Phys. Rev. A* **46** 3846